

Structure functions in decomposing CuRh systems

M. Prem and O. Blaschko

*Institut für Experimentalphysik, Universität Wien, Strudlhofgasse 4, A-1090 Wien, Austria
and Laboratoire Léon Brillouin, Centre d'Etudes Nucléaires de Saclay, F-91191 Gif sur Yvette, France*

L. Rosta

Research Institute for Solid State Physics, H-1525 Budapest, Hungary

(Received 10 June 1996)

The time evolution of a CuRh alloy quenched within the miscibility gap is investigated by small and wide angle neutron scattering techniques. Near fundamental Bragg reflections diffuse satellites arising from a lattice parameter modulation induced by the precipitation pattern are investigated. The results show that in CuRh the precipitation morphology and its time evolution are quite different from decomposition characteristics recently observed in the system AuPt. The results are discussed and related to the larger lattice misfit present in CuRh in comparison to AuPt. [S0163-1829(97)01405-7]

I. INTRODUCTION

In recent years the characteristics of structure functions during the decomposition of alloys were the subject of both theoretical and experimental investigations. Knowledge of the width and the shape of the structure function gives insight into the evolution of atomic correlations occurring during a decomposition process.^{1,2}

Both theoretical investigations and computer experiments show that during the late stages of decomposition a scaling law holds for the evolution of the mesoscopic precipitation pattern whose time evolution can consequently be described by a single time dependent length.^{3,4} In scattering experiments the decomposition process is analyzed in terms of the time dependent structure function $S(Q, t)$ which likewise shows scaling behavior.⁵⁻¹⁰

In solid state systems the morphology of the precipitation pattern is generally influenced by the presence of elastic interactions. In some alloys characterized by a lattice misfit of a few percent between the solid solution and the precipitated phases the decomposition process induces a long range modulated precipitation structure consisting of a periodic arrangement of platelets of the new phases.¹¹⁻¹⁶ This modulated precipitation structure induces the appearance of satellites (or sidebands) near fundamental Bragg reflections.^{16,17}

In a recent paper the decomposition characteristics were investigated in a AuPt system for a series of concentrations within the miscibility gap.¹⁸ The measurements were performed by neutron scattering techniques, i.e., the small angle scattering and the intensities occurring at sideband positions near fundamental Bragg reflections were investigated during the decomposition process. A main result of this investigation was that the sideband intensity had a similar functional shape as the intensity distribution observed in the small angle scattering experiment. It followed that the lattice parameter modulation which gives rise to the satellite intensities is similar to the modulation of the atomic concentration which is seen in the small angle scattering experiment. Moreover, in the symmetric AuPt alloy a rather sharp structure function exhibiting a shoulder near the second order position is ob-

served. Both features, i.e., the sharpness of the structure function and the intensity shoulder, indicate that the modulated precipitation pattern which consists of a sequence of alternating Au and Pt-rich platelets lying on (002) lattice planes induces long range atomic correlations. Furthermore, in the symmetric AuPt system the modulated precipitation pattern seems to be rather stable with respect to annealing treatments and no classical $t^{1/3}$ growth law was observed. In the middle of the miscibility gap the system exhibits a very slow time evolution of the form $t^{1/m}$ with m yielding values near 100. This time dependence may also be described by a logarithmic growth law. However, the essential fact is that in symmetric AuPt the time dependence is nearly arrested.

The results of the AuPt system therefore indicate that in order to reduce the elastic energy of the system the presence of a finite lattice misfit induces the formation of a long range modulated structure consisting of platelets of Au and Pt with coherent interfaces. Moreover this structure is rather stable and its time evolution is drastically slowed down.

On the other hand, systems exhibiting modulated lamellar structures with accompanying sideband intensities are known from the literature only to occur for a lattice misfit up to a certain size. For larger misfits no sideband intensities are reported during the decomposition process and it seems therefore that a coherent modulated structure is stable only within a finite misfit range.

The question arises what changes of the precipitation pattern occur when the lattice misfit is further increased in a decomposing system. In order to investigate this question we performed neutron scattering measurements of the decomposition in a CuRh alloy. CuRh has a similar phase diagram as AuPt with a large miscibility gap but exhibits a significantly larger lattice misfit between the precipitation phases (misfit $\Delta a/a$ is 0.0316 and 0.0367 in AuPt and CuRh, respectively, where a is the lattice parameter of the solid solution).

II. EXPERIMENT

The starting material was a polycrystalline CuRh alloy with three different concentrations, i.e., Cu₇₅Rh₂₅,

$\text{Cu}_{50}\text{Rh}_{50}$, and $\text{Cu}_{20}\text{Rh}_{80}$. From this material platelets with a typical size of $10 \times 10 \times 1$ mm were cut and submitted to a homogenization treatment for several hours at 1200°C . After two homogenization treatments some of the polycrystalline samples had become single crystals. The neutron scattering measurements were performed on these single crystals. After the homogenization treatment the platelets were quenched into water and annealed especially at 600°C where the CuRh system shows a significant time evolution within a reasonable time range. At lower temperatures the time evolution is too slow and at higher temperatures too fast in order to be able to investigate many different annealing times.

The small angle scattering measurements were done on the spectrometer PAXE of the Laboratoire Léon Brillouin in Saclay. Incident neutron wavelengths of 8 and 4 \AA were used. The intensities occurring near satellite positions during the decomposition were measured on the conventional triple axis spectrometer VALSE located on a cold neutron guide position.

The measurements were finally performed on the $\text{Cu}_{75}\text{Rh}_{25}$ and $\text{Cu}_{50}\text{Rh}_{50}$ samples. Due to the high neutron absorption of Rh samples with a thickness of only a few tenths of a mm were required for the Rh-rich $\text{Cu}_{20}\text{Rh}_{80}$ alloy which inevitably broke during the preparation.

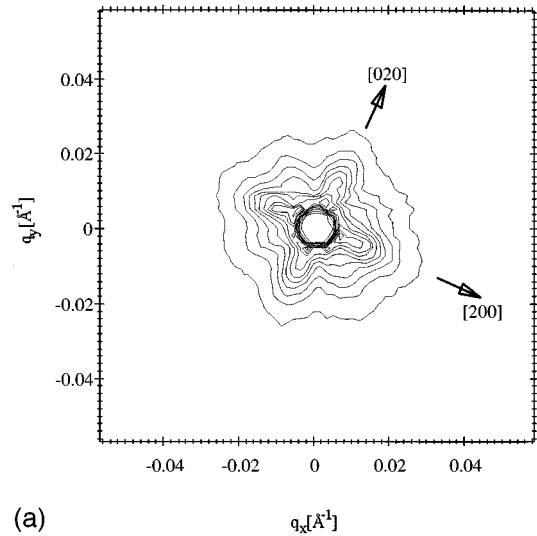
III. RESULTS

A typical small angle scattering pattern as obtained from the Cu-rich $\text{Cu}_{75}\text{Rh}_{25}$ alloy annealed at 600°C for 24 h is shown in Fig. 1(a). The figure shows intensity lobes along $[002]$ fcc directions.

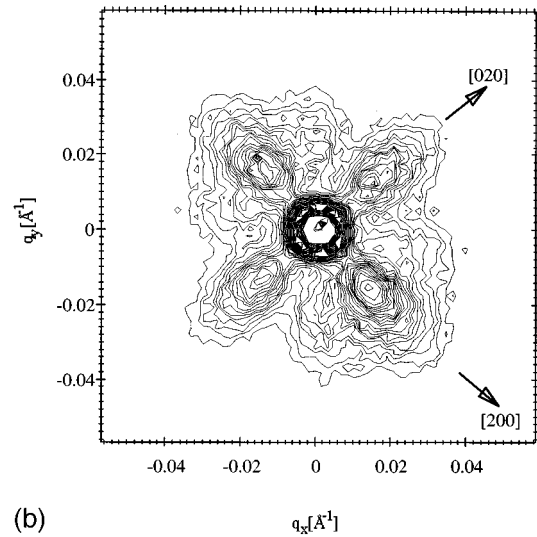
An experiment with a similar $\text{Cu}_{75}\text{Rh}_{25}$ sample annealed at 700°C for 1 h gave an intensity pattern likewise showing pronounced streaks along cubic $[002]$ directions [Fig. 1(b)].

From basic arguments of scattering theory¹⁹ it follows that intensity streaks along $[002]$ directions indicate the presence of platelike precipitates lying on (200) planes of the fcc lattice. In the dilute Cu-rich alloy the measurements therefore indicate a platelike morphology of the Rh-rich precipitates within the fcc matrix. This finding is in general agreement with theoretical considerations predicting the formation of plate-shaped precipitates under equilibrium conditions in cases of large elastic strain energies.^{20,23,16}

On the other hand, contrary to expectations, in the symmetric CuRh system the small angle scattering patterns give no indication of intensity streaks (Fig. 2). The isointensity contours are essentially characterized by a square shape and especially the outer contours do not show any protrusions along $[002]$. The measured intensity distributions for all annealing times at 600°C always show peaks located on $[002]$ fcc directions and no intensity streaking is observed even after annealing treatments of 32 h at 600°C (Fig. 2). The four intensity maxima on $[002]$ fcc directions indicate that the precipitates are located on crystallographic $[002]$ directions. The square appearance of the small angle scattering pattern is observed within a well-defined reciprocal lattice plane, i.e., $[002]$ reciprocal lattice plane as easily seen from Fig. 2(b). Cube-shaped precipitates with cube axes along $[002]$ fcc directions induce a square appearance of intensity contours in the $[002]$ reciprocal lattice plane.



(a)



(b)

FIG. 1. Two-dimensional small angle scattering distribution represented by equally spaced isointensity contours. (a) $\text{Cu}_{75}\text{Rh}_{25}$ annealed at 600°C for 24 h. (b) The same alloy annealed at 700°C for 1 h.

The absence of any streaking along $[002]$ in the symmetric CuRh alloy is a scattering feature significantly different from that found in the dilute Cu-rich $\text{Cu}_{75}\text{Rh}_{25}$ alloy. Moreover, the CuRh results are also quite different from that previously found in a symmetric AuPt system where pronounced intensity streaks along $[002]$ directions were observed [for comparison the previous results of AuPt are included in Fig. 2(c)].

From the measured intensity distributions the structure functions $S(Q, t)$ were evaluated. Figure 3 shows the results for a series of annealing treatments at 600°C . The figure indicates that in the symmetric alloy the intensity distribution shifts towards smaller Q values with increasing annealing time. It follows that in the symmetric CuRh system coarsening occurs at 600°C . An analysis shows that the time evolution of $1/Q_{\text{max}}$ (Q_{max} gives the position of the intensity maximum) is in accordance with a classical $t^{1/3}$ dependence²⁴ (see Fig. 4).

Furthermore, the dynamic scaling behavior of the struc-

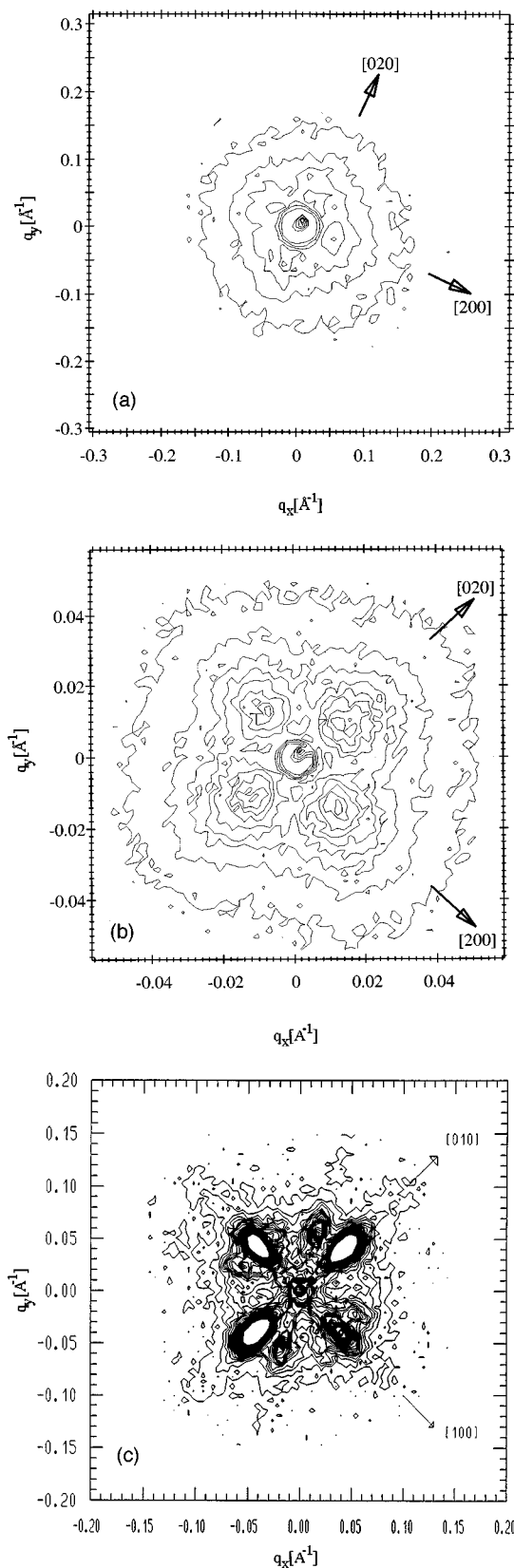


FIG. 2. Two-dimensional small angle scattering distribution observed in the symmetric CuRh system annealed at 600 °C: (a) 1 h; (b) 32 h; (c) for comparison the previous results of Au₄₀Pt₆₀ annealed at 600 °C are included exhibiting a pronounced streaking along [001]-fcc directions.

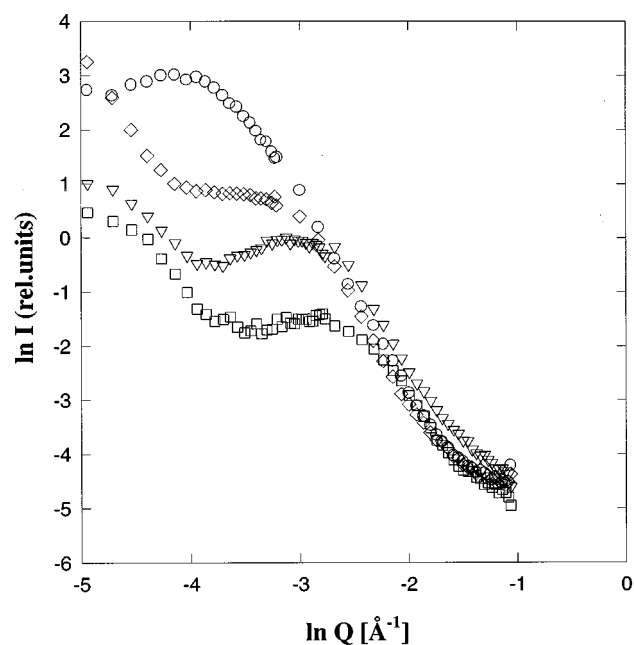


FIG. 3. Time evolution of the spherically averaged small angle scattering intensity observed in the symmetric alloy Cu₅₀Rh₅₀ during annealing at 600 °C for 1 h (squares), 4 h (triangles), 8 h (diamonds), and 32 h (circles).

ture functions was analyzed following the general relation^{6,7}

$$S(Q, t) = VR^d F(x).$$

$F(x)$ is a time-independent scaling function where $x = QR$. R is a typical length scale characterizing the precipitation pattern. V is the integrated intensity which is related to the total clustered volume and d is the dimension of the system. R may be related to Q_{\max} ($R \sim 1/Q_{\max}$), where Q_{\max} is the value which maximizes the structure function.

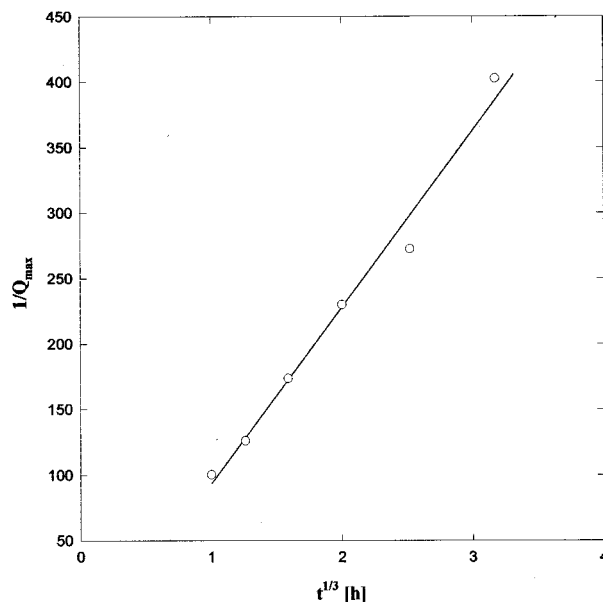


FIG. 4. $1/Q_{\max}$ versus time in the symmetric alloy Cu₅₀Rh₅₀ during annealing at 600 °C.

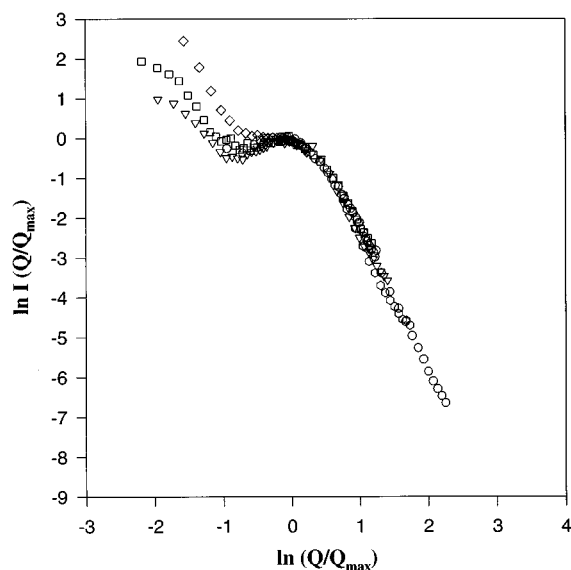


FIG. 5. The scaled structure function in the symmetric CuRh system as determined from the small angle scattering data. The symbols are the same as in Fig. 3. Experimentally observed structure functions generally show a scatter of the data at very small Q values where the data are contaminated by the presence of the direct beam. These data points were included to show the validity range, however, from this Q range no information can be deduced. Outside this range all data points are represented by a single curve.

The scaled intensity distributions are represented in Fig. 5 showing as a general behavior that all measured intensity distributions can be represented by a single scaled structure function. The scaled function, however, is rather broad and no intensity shoulder is observed in the data.

Moreover, the elastic diffuse intensities occurring near fundamental Bragg reflections were measured in the same series of CuRh alloys as a function of annealing time at 600 °C. A typical result is shown in Fig. 6 after an annealing time of 1 h. The figure gives evidence for diffuse satellites and therefore indicates, as expected, the presence of a lattice parameter modulation in the annealed alloy. The measured satellite intensities were analyzed in terms of the above mentioned scaling relation and the results were compared to the small angle scattering data (Fig. 7). The comparison shows that the scaled satellite intensities and the scaled small angle scattering data are similar and can again be represented by a single curve.

IV. DISCUSSION

First, the present experimental data show that in the dilute $\text{Cu}_{75}\text{Rh}_{25}$ alloy the precipitation occurs into plates parallel to (002) fcc matrix planes. This result is in agreement with theoretical treatments predicting plates as equilibrium shape of the precipitates in cases of large elastic strain energies.

Secondly, in the symmetric CuRh system precipitates are aligned along (002) fcc matrix directions as borne out by the location of the intensity peaks in the small angle scattering patterns. During annealing the precipitation pattern shows coarsening in accordance with the classical Lifshitz-Slyozov $t^{1/3}$ behavior. However, the absence of any streaking in the

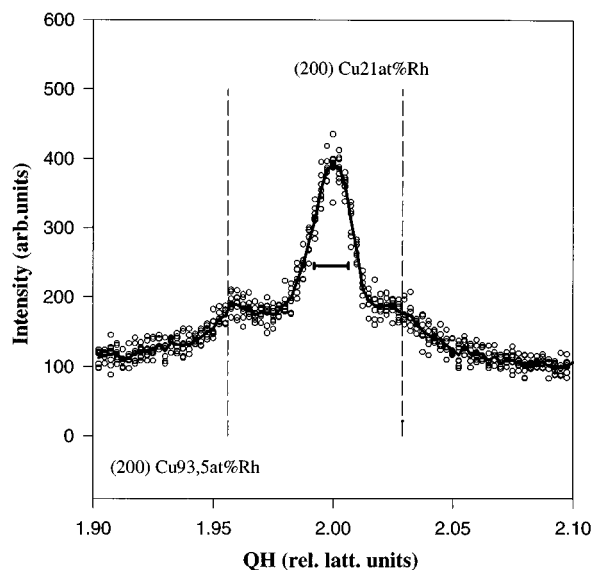


FIG. 6. Sideband scattering near the (200) fundamental reflection measured in $\text{Cu}_{50}\text{Rh}_{50}$ after annealing at 600 °C for 1 h. The horizontal bar indicates the measured width in the as-quenched alloy representing the experimental resolution. The dashed vertical lines indicate the expected positions of the (200) reflections of the Cu-rich and Rh-rich precipitated phases, respectively. The background is flat.

scattering pattern provides evidence that no platelike precipitates are formed in the symmetric CuRh alloy. From the squared shape of the iso-intensity contours observed within the (100) scattering plane (Fig. 2) it can be concluded that the mean shape of the precipitates may be described by cubes whose cubic axes are aligned along [001] fcc directions.

Moreover, the scaled structure function in CuRh is drastically broader compared to that observed in AuPt and does not show any shoulder at the second order position. It fol-

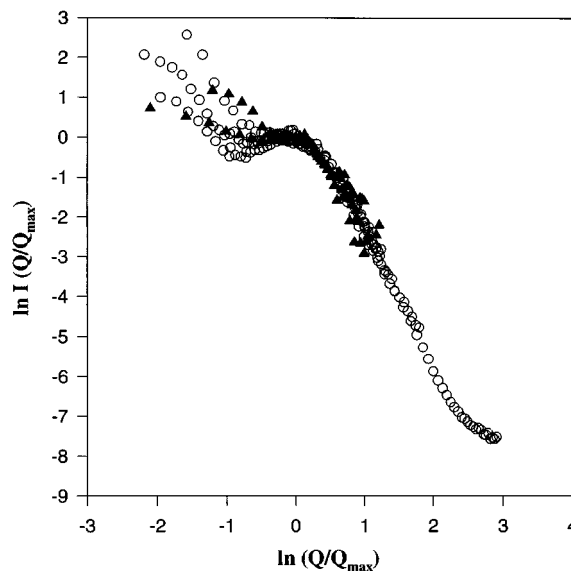


FIG. 7. The scaled structure function evaluated from the sideband scattering in $\text{Cu}_{50}\text{Rh}_{50}$ (filled symbols) in comparison to the structure function of Fig. 5 (open symbols).

lows that the long range atomic correlations in CuRh are less pronounced than in the AuPt system. The observed width of the structure function in CuRh is even somewhat larger than that measured in a melt-spun AuPt alloy where the finite grain size inhibits the formation of a long range modulated structure.^{18,25}

Furthermore, satellite intensities near fundamental matrix reflections are likewise found in CuRh. The intensity distribution of the satellites is similar to the intensity distribution observed in the small-angle scattering experiment, i.e., the scaled intensity distributions obtained from the small-angle scattering experiment and from the satellite intensities can be represented by the same curve. The small angle scattering technique investigates fluctuations and modulations of the atomic concentration whereas the sideband scattering essentially arises from a modulation of the lattice parameter. From the similar functional shape of the scattering observed at small and high Q values it follows that the modulation of the atomic concentration and of the lattice parameter are similar in the decomposed system.

The precipitation morphology in the symmetric CuRh system appears to be significantly different from that found previously in the symmetric AuPt alloy. In AuPt a coherent configuration of parallel plates inducing long range atomic correlations was found. In CuRh the precipitation pattern consists of an arrangement of cuboid precipitates alternatingly rich in Cu and Rh where the atomic correlations are of much shorter range as borne out by the broader structure function.

These findings should be related to the different lattice misfits in the two systems. The experimental results indicate that in symmetric alloys a further increase of the lattice misfit induces a transformation within the mesoscopic precipitation pattern, i.e., from a long-range modulated coherent structure (AuPt) consisting of parallel plates to an arrangement of cuboid precipitates where the long range correlations are drastically reduced (CuRh).

This observation of such a behavior seems to be at variance with theoretical treatments showing that in the case of large lattice misfit and consequently large elastic strain the equilibrium shape of precipitates should be a plate which is characterized by a lower elastic energy.^{20–22} These treatments deal, however, with the behavior of isolated particles within the matrix and do not consider a modulated structure as a structural entity of its own. Moreover, most experimental work was performed on systems showing a significant smaller lattice misfit ($\sim 1\%$) than the present CuRh alloy.^{15,16,26}

Within a modulated structure a significant contribution to the elastic energy of the system arises from the coherent interfaces between, e.g., Au-rich and Pt-rich platelets. If a coherent interface is present the lattice misfit has to be accommodated by elastic strain within the interface region. The accommodation of the interfaces by elastic strain is easier if the lattice misfit is small. If the misfit is increased it may no longer be accommodated by elastic deformation alone but plastic deformation may occur and the coherency between the interfaces is lost. Therefore, in symmetric CuRh the modulated structure appears to be no more coherent at the interfaces between the Cu-rich and Rh-rich regions thus implying the occurrence of plastic deformation. The broadening

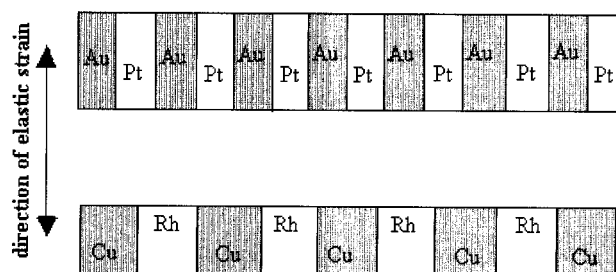


FIG. 8. Schematic representation of the transition in the modulated structure observed with increasing lattice misfit between the AuPt and CuRh systems. The figure is not drawn to scale. Along the horizontal axis of the figure the lattice misfit is compensated by the alternating sequence of Cu-rich and Rh-rich (or Au-rich and Pt-rich) precipitates. The main elastic strains occur perpendicularly to the axis of modulation. The modulated structure as a whole may be considered as one precipitate creating a strain field with cylindrical symmetry around the axis of modulation. With increasing lattice misfit the strain energy can be decreased by reducing the lateral dimensions of the modulated structure as observed in this experiment.

of the (002) matrix reflection shown in Fig. 6 with respect to the measured resolution (horizontal bar in the figure) confirms that plastic deformation has occurred during decomposition. The plastic deformation and the loss of coherency deteriorates the long range correlation of the modulated structure thus inducing the significant broadening of the structure function as observed. Moreover, the loss of coherency seems to facilitate processes of atomic diffusion at the interfaces which are responsible for the observed $\sim t^{1/3}$ coarsening of the modulated structure.

The most peculiar result of this investigation is the absence of platelike precipitates in the symmetric CuRh alloy which is in contrast to the results of AuPt and is not expected by theoretical work based on elastic strain energy considerations.

First, it may be argued that if plastic deformation occurs during decomposition general results obtained from considerations about elastic strain energies alone may not apply.

Secondly, it can be seen that a coherent modulated structure consisting of alternating plates breaks up at the coherent interfaces when the lattice misfit increases. From this consideration it may be conjectured that an arrangement of alternating coherent plates is not a favorable configuration in cases of large lattice misfit.

The transition in the mesoscopic precipitation pattern found between the AuPt and CuRh system is schematically shown in Fig. 8. Both structures induce zero strain along the axis of modulation (horizontal axis in the figure), i.e., in a sequence of alternating precipitates (e.g., Au-rich and Pt-rich or Cu-rich and Rh-rich) the variation of the lattice parameter is compensated along the axis of the modulation.

On the other hand, perpendicularly to the modulation axis both systems induce elastic strain in the matrix. This elastic strain may be reduced if the lateral dimensions of the platelets within the modulated structure are likewise reduced. It follows that a transition from a configuration shown in Fig. 8(a) to that depicted in Fig. 8(b) may result in agreement with the present experimental observation.

In summary, the present investigation confirms that in the dilute $\text{Cu}_{75}\text{Rh}_{25}$ alloy the precipitates are plates in accordance with theoretical expectations. On the other hand, in the symmetric CuRh system a modulated structure is found showing, however, long range atomic correlations which are significantly reduced with respect to that previously observed in a AuPt system. The measurements in symmetric CuRh give no evidence of the formation of precipitation plates within the modulated structure. The present results rather indicate that a coherent arrangement of parallel plates of al-

ternating atomic concentrations becomes unstable if the lattice misfit is increased, i.e., the coherency and the long-range atomic correlations related to it are reduced within the modulated precipitation structure.

ACKNOWLEDGMENTS

Our work was partly supported by the Fonds zur Förderung der wissenschaftlichen Forschung in Austria. We thank A. Lovas and J. Takacs for sample preparation.

-
- ¹J. D. Gunton, M. San Miguel, and P. S. Sahni, in *Phase Transition and Critical Phenomena*, edited by C. Domb and J. L. Lebowitz (Academic, New York, 1983), Vol. 8.
 - ²G. Kosterz, Phys. Scr. **T49**, 636 (1993).
 - ³K. Binder, M. H. Kalos, J. L. Lebowitz, and J. Marro, Colloid Interface Sci. **10**, 173 (1979).
 - ⁴S. Komura, Phase Transit. **12**, 173 (1979).
 - ⁵S. Komura, K. Osamura, H. Fuji, and T. Takeda, Phys. Rev. B **39**, 2944 (1984).
 - ⁶J. Marro, J. L. Lebowitz, and M. H. Kalos, Phys. Rev. Lett. **43**, 282 (1979).
 - ⁷P. Fratzl, J. L. Lebowitz, J. Marro, and M. H. Kalos, Acta Metall. **31**, 1849 (1983).
 - ⁸M. Hennion, D. Ronzaud, and P. Guyot, Acta Metall. **30**, 599 (1982).
 - ⁹O. Blaschko and P. Fratzl, Phys. Rev. Lett. **51**, 288 (1983).
 - ¹⁰O. Blaschko, R. Glas, and P. Weinzierl, Acta Metall. Mater. **38**, 1053 (1990).
 - ¹¹V. Daniel and H. Lipson, Proc. R. Soc. London Ser. A **181**, 368 (1943).
 - ¹²M. E. Hargreaves, Acta Crystallogr. **4**, 301 (1951).
 - ¹³A. Guinier, Acta Metall. **3**, 510 (1955).
 - ¹⁴A. Guinier, in *Solid State Physics*, edited by H. Ehrenreich, F. Seitz, and D. Turnbull (Academic, New York, 1959), Vol. 9, p. 293.
 - ¹⁵J. Manenc, Acta Metall. **7**, 124 (1959).
 - ¹⁶A. J. Ardell, R. B. Nicholson, and J. D. Eshelby, Acta Metall. **14**, 1295 (1966).
 - ¹⁷T. Tsujimoto, K. Hashimoto, and K. Saito, Acta Metall. **25**, 295 (1977).
 - ¹⁸R. Glas, O. Blaschko, and L. Rosta, Phys. Rev. B **46**, 5972 (1992).
 - ¹⁹J. M. Cowley, *Diffraction Physics* (North-Holland, Amsterdam, 1995).
 - ²⁰F. R. N. Nabarro, Proc. Phys. Soc. London **52**, 90 (1940).
 - ²¹A. G. Khachaturyan, *Theory of Structural Transformations in Solids* (Wiley, New York, 1983).
 - ²²Yunzhi Wang, Long-Quing Chen, and A. G. Khachaturyan, Scr. Metall. Mater. **25**, 1969 (1991).
 - ²³Long-Qing Chen, Yunzhi Wang, and A. G. Khachaturyan, Philos. Mag. Lett. **64**, 241 (1991).
 - ²⁴L. M. Lifshitz and V. V. Slyozov, J. Phys. Chem. Solids **19**, 35 (1961).
 - ²⁵S. P. Singhal, H. Herman, and G. Kosterz, J. Appl. Crystallogr. **11**, 572 (1978).
 - ²⁶M. Fährmann, P. Fratzl, E. Fährmann, and William C. Johnson, Acta Metall. Mater. **43**, 1007 (1995).